

# Cluster Amplitudes and Their Interplay with Self-Consistency in Density Functional Methods

Greta Jacobson,<sup>1,2</sup> Juan M. Marmolejo-Tejada,<sup>1</sup> Martín A. Mosquera<sup>1,\*</sup>

<sup>1</sup>Department of Chemistry and Biochemistry, Montana State University, Bozeman, Montana 59717 USA

<sup>2</sup>Department of Chemistry, Millikin University, Decatur, Illinois 62522 USA

\* [martinmosquera@montana.edu](mailto:martinmosquera@montana.edu)

August, 2022

## Abstract

Density functional theory (DFT) provides convenient electronic structure methods for the study of molecular systems and materials. Regular Kohn-Sham DFT calculations rely on unitary transformations to determine the ground-state electronic density, ground state energy, and related properties. However, for dissociation of molecular systems into open-shell fragments, due to the self-interaction error present in a large number of density functional approximations, the self-consistent procedure based on the this type of transformation gives rise to the well-known charge delocalization problem. To avoid this issue, we showed previously that the cluster operator of coupled-cluster theory can be utilized within the context of DFT to solve in an alternative and approximate fashion the ground-state self-consistent problem. This work further examines the application of the singles cluster operator to molecular ground state calculations. Two approximations are derived and explored: i), A linearized scheme of the quadratic equation used to determine the cluster amplitudes, and, ii), the effect of carrying the calculations in a non-self-consistent field fashion. These approaches are found to be capable of improving the energy and density of the system and are quite stable in either case. The theoretical framework discussed in this work could be used to describe, with an added flexibility, quantum systems that display challenging features and require expanded theoretical methods.

## 1 Introduction

Electronic structure methods predict a very large number of measurable quantities that are used to understand, characterize, and optimize chemical compounds and materials. Quantum mechanics is the foundation upon which algorithms are designed and applied to compute electronic and structural properties. From a fundamental standpoint, quantum mechanics states that with a complete knowledge

of the wave function of the system one can thus be able to determine all the information about the system of interest. For computational efficiency, however, density functional theory (DFT) serves as an alternative to pursue such goal. In DFT one the primary objectives is the calculation of the electronic density of the system, as opposed to the full wave function of all the electrons. Although it is common to separate both, wave-function theory (WFT) and DFT, as separate fields, it can be argued that both are intrinsically connected, especially from the algorithmic point of view.

DFT methods have been formulated on the basis of physical understanding of model systems and small molecules. A notable example is the electron gas, which in many ways has led to functional components that to date still remain an important part of a very large number of density functional approximations (DFAs). These functionals are available for different energy “pieces” such as the kinetic, exchange, correlation, and van der Waals energies. The kinetic energy is known to be the most challenging energy to be expressed explicitly as a density-functional. For this reason, Kohn-Sham (KS) DFT [1] is the most common theory within DFT that is utilized for practical calculations and to derive concepts.[2, 3] As KS-DFT uses single-electron orbitals to determine a kinetic energy. As is well known, even though KS-DFT practical calculations perform well for determining properties such as molecular geometries, and optoelectronic properties of a very large number of compound types, it is difficult for transition-metal systems [4], bond-breaking [5], and charge-transfer excitations [6], among others, where erroneous charge delocalization [7–10] is a main manifestation of these adverse effects.

Extended DFAs that are free of incorrect charge delocalization should eliminate the main cause for such adverse effect, the self-interaction error [11–14]. Additionally, improved methodologies must also come with relatively low computational costs. Motivated by these considerations, and fueled by advances in machine learning and the premise of new generation of computing technologies (classical and quantum), theoretical methods are being advanced by the scientific community, with the goal of extending the applicability of DFT methods [15–17]. These extensions include the development of force fields, which are creating opportunities for detailed studies of systems at the mesoscopic scale [18]. For example, artificial neural network (ANN) algorithms have been used to generate density functional approximations [19, 20], and have been able to eliminate charge delocalization errors. On the other hand, ANNs also have led to both transferable and specific force fields. This also includes ANNs being used extensively in materials discovery and properties prediction [21–23]. Machine-learned interatomic potentials, which are tailored for a particular system of interest demonstrate quite appealing theoretical prospects for modeling mesoscale phenomena [24–30].

From a foundational perspective, the elimination of charge delocalization still remains a long sought goal, where theoretical tools are still the subject of continued developments. This problem not only manifests in DFT development, but also in WFT research. For example, it is known that there are dynamically correlated post-Hartree-Fock methods that can also cause issues with size-consistency, whereas the well-known exponential ansatz of WFT, in conjunction with spin-symmetry breaking, offers a theoretically sound route to restore size-consistency (which implies size-extensivity as well). We showed previously that this exponential operator, which in turn is determined by what is known

as the “cluster operator” [31–41], can also prevent undesired charge delocalization in DFT calculations [42]. The cluster operator in the ground-state case is limited in our calculations to single-electron transitions, as it displays a high degree of accuracy at this level of excitation. The cluster amplitudes that are used to construct the exponential operator are derived as the solution of a quadratic equation, which is solved in an iterative fashion. Our proposed method, denoted as “eXp” (due to its relying on the exponential operator), predicted with physical consistency the binding energy curves of classical systems such as di-hydrogen, lithium hydride, and hydrogen fluoride, but we also show other cases where the eXp method functions as an alternative to the standard unitary method of KS-DFAs, and we suggested they are also compatible with the double-hybrid functional approach [43–45]. These previous findings motivate the present work, where we further explore the eXp method under its linearized version, which simplifies in a very accurate way the determination of the cluster amplitudes and the exponential operator. We also examine non-self-consistent field calculations, where the single-particle Hamiltonian is determined by the Hartree-Fock density, which is used to estimate directly the cluster operator and its conjugate, the “lambda” operator. In this study we find that the linearized eXp method performs quite well with excellent agreement with respect to the full quadratic scheme in both cases, the self-consistent and the non-self-consistent ones. The eXp technique is applied to a couple of known cases of severe charge delocalization (or strong self-interaction), with the goal of eliminating it: The positively charged neon dimer,  $\text{Ne}_2^+$ , and lithium-fluoride, LiF. In addition, our methods are applied to a set of molecules at their minimum-energy geometries, where we show that the linearized eXp method performs quite similarly as the quadratic version in self-consistent-field (SCF) and *non*-self-consistent-field (NSCF) calculations. However, the NSCF computations, as expected, are less accurate than the SCF ones, but can be considered for calculations where computational acceleration is needed. The simulations considered in this work are based on a single-particle Hamiltonian, but they are also applicable to Hamiltonians that include two-body interactions, such as those used in double-hybrid approaches.

## 2 Theory

## 3 Computational Details

Determining ground-state properties in KS-DFT begins with the calculation of the KS Slater determinant  $|\Phi\rangle$  and subsequently the electronic energy. The wave function  $|\Phi\rangle$  is computed through the minimization of an auxiliary single-particle energy, which depends on the single-particle Hamiltonian, or KS Fock operator. We denote this density-dependent operator as  $\hat{f}$ . The energy function that is minimized in KS-DFT to obtain the orbitals is then  $\langle\Phi|\hat{f}|\Phi\rangle$ , and it leads to the standard KS equations where the single particle orbitals are constructed through diagonalization of the KS Fock matrix. The object  $\hat{f}$  is the sum of the kinetic, electron-nucleus, exchange-correlation (XC), and Hartree contributions.

As an alternative to the standard procedure mentioned above, we stationarize the single-particle energy with respect to cluster operators, where the reference is a Hartree-Fock (HF) wave function, which we denote as  $\Psi_0$ . This wavefunction, as expected, is constructed with occupied orbitals in the HF molecular orbital basis set. This is a relevant detail, as our calculations rely entirely on such molecular basis set. The HF wavefunction can either be a restricted or unrestricted reference. We introduce an auxiliary right-handed wave function of the form  $|\Upsilon_R\rangle = \exp(+\hat{t})|\Psi_0\rangle$ , and the left-ket  $\langle\Upsilon_L| = \langle\Psi_0|(1 + \hat{\Lambda})\exp(-\hat{t})$ , where  $\hat{t}$  and  $\hat{\Lambda}$  are the cluster operators. The function to stationarize is  $\langle\Upsilon_L|\hat{f}|\Upsilon_R\rangle$ , so it leads to the auxiliary single-particle energy as:

$$E_s = \text{stat.}_{\hat{t}, \hat{\Lambda}} \langle\Psi_0|(1 + \hat{\Lambda})\bar{f}|\Psi_0\rangle \quad (1)$$

where the symbol  $\bar{f}$  denotes the transformed operator  $\exp(-\hat{t})\hat{f}\exp(+\hat{t})$ . We use this notation for other operators too; so if  $\hat{\Omega}$  is some arbitrary operator, then  $\bar{\Omega} = \exp(-\hat{t})\hat{\Omega}\exp(+\hat{t})$ . The cluster operators that we are interested in have the form  $\hat{t} = \sum_{ai} t_i^a \hat{a}^\dagger \hat{i}$ , and  $\hat{\Lambda} = \sum_{ai} \Lambda_i^a \hat{i}^\dagger \hat{a}$ . The indices  $i$  and  $a$  denote occupied and virtual spin-orbitals, respectively. By stationarizing with respect to  $\hat{t}$  and  $\hat{\Lambda}$  it is then implied that one must find, what we regard as vectors computationally,  $\{t_i^a\}$  and  $\{\Lambda_i^a\}$ . This demands that the derivatives of the function  $\langle\Psi_0|(1 + \hat{\Lambda})\bar{f}|\Psi_0\rangle$  with respect to all the elements  $\Lambda_i^a$  and  $t_i^a$  are all zero.

We denote  $f_{pq}$  as the matrix element,  $\langle\chi_p|\hat{f}|\chi_q\rangle$ , where  $\chi_p$  is a *Hartree-Fock spin-orbital*; this implies that  $f_{pq}$  can be non-zero for  $p \neq q$ . We then have that the  $t$ -amplitudes derive from the equation:

$$0 = f_{ai} + \sum_b t_i^b f_{ab} - \sum_j t_j^a f_{ji} - \sum_{jb} f_{jb} t_i^b t_j^a \quad (2)$$

And the  $\Lambda$ -amplitudes are obtained from the linear system  $\mathbf{M}\mathbf{\Lambda} = -\mathbf{f}$ , where

$$M_{ck,ai} = R_{ck,ai} - \sum_j t_j^a f_{jc} - \sum_b t_i^b f_{kb} \delta_{ac} \quad (3)$$

and

$$R_{ck,ai} = f_{ca} \delta_{ik} - f_{ki} \delta_{ca} \quad (4)$$

The symbol  $\mathbf{f}$  represents the Fock matrix as a vector,  $(\mathbf{f})_{ai} = f_{ai}$ . We denote the process of determining  $\mathbf{t}$  through Eq. 2 as the quadratic eXp scheme, or ‘‘Q-eXp’’. It, Q-eXp, can be solved using the quasi-Newton method where an estimate to  $t_i^a$  is updated according to the equation:

$$t_i^a \leftarrow t_i^a - \frac{L_i^a}{f_{aa} - f_{ii}} \quad (5)$$

Where  $L_i^a$  refers to the left-hand side of Equation 2.

By neglecting quadratic terms in Eq. 2, we obtain the approximation:

$$\mathbf{Rt} = -\mathbf{f} \quad (6)$$

We refer to this scheme as ‘‘L-eXp’’. This approximation requires the solution to a linear system of equations, so it avoids the need for iterations to find  $t$ . On the other hand, this linear matrix equation

can be further reduced to the simple, approximated, analytical expression:  $t_i^a = -f_{ai}/(f_{aa} - f_{ii})$ , which we used before as a first estimate to start a the iterative cycle in Q-eXp. In this work we explore the L-eXp and Q-eXp methods in NSCF and SCF procedures. So NSCF L-eXp, for instance, refers to the use of the linearized eXp method, Eq. 6, where the amplitudes are computed only one time, and the XC and Hartree potentials are evaluated at the Hartree-Fock densities; the same applies to NSCF Q-eXp.

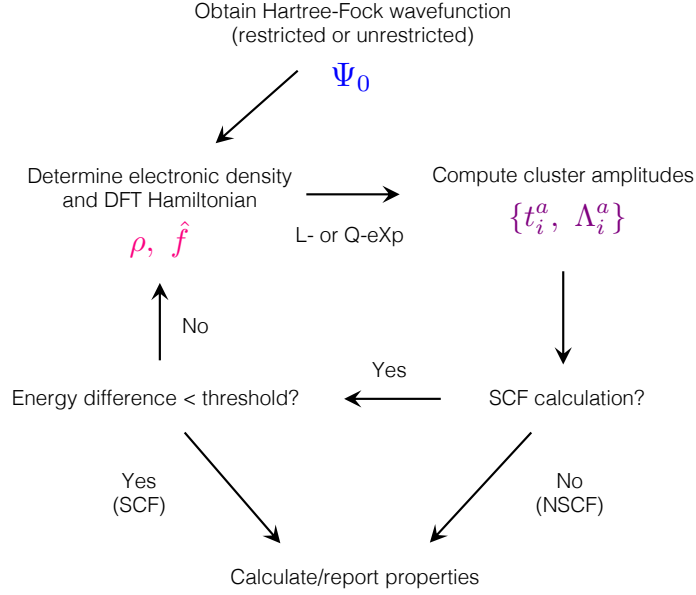


Figure 1: Flow chart summarizing steps carried out in a single-point calculation based on an eXp method (linear or quadratic). The cluster amplitudes are determined with respect to the Hartree-Fock reference and molecular basis.

Given the solution to the above problems the energy is calculated as:

$$E = \langle \Psi_0 | (1 + \hat{\Lambda}) e^{-\hat{t}} \hat{h}_0 e^{+\hat{t}} | \Psi_0 \rangle + E_{\text{Hxc}}[\rho] \quad (7)$$

where  $\hat{h}_0$  is the core Hamiltonian (kinetic plus electron-nuclei attraction energy operators), and  $\rho(\mathbf{r}) = \langle (1 + \hat{\Lambda}) \bar{\rho}(\mathbf{r}) \rangle$ . The term  $E_{\text{Hxc}}$  refers to the sum of the Hartree and XC energies, where the XC energy is approximated with a DFA. The steps followed to calculate the ground-state energy, and related properties are summarized in Figure 1. As usual, in the SCF cycle the electronic density is updated until the energy variation between iterations is below a certain threshold. In the NSCF approach the cluster amplitudes are only determined one time, with the Fock operator being based on the (U)HF electronic density, or density matrix if the XC functional is hybridized.

An important quantity in our calculation is the fundamental energy gap of the system, as our iterations depend on differences of the type  $f_{aa} - f_{ii}$ , at moderately long distances a few of these

can be close to zero, which cause instabilities. To eliminate them, we use a regularization scheme in which the Fock operator is modified by the  $t$  cluster amplitudes, so the new operator is  $\hat{f}_\alpha = \hat{f} + \alpha \hat{t}$ , where the regularization number  $\alpha > 0$ , and the problem is solved with respect to such single-particle Hamiltonian, otherwise the methodology remains the same. In Ref. [42] we show details of this regularization procedure. For the quadratic method Q-eXp, in Eq. (5) the difference  $f_{aa} - f_{ii}$  is replaced by  $f_{aa} - f_{ii} + \alpha$  and the term  $L_i^a$  by  $L_i^a + \alpha t_i^a$ . For the linearized eXp method, we just add the constant  $\alpha$  to all the diagonal elements of the matrix  $\mathbf{R}$ . Around minimum-energy, or equilibrium, geometries we do not find a need to use such regularization scheme, but there are other cases where this is necessary. Regularization is a benign procedure that eliminates instabilities and is used in standard coupled-cluster [46–49], perturbative theories [50, 51], multireference methods [52], and related theories such as pseudo-potentials and machine-learning.

## 4 Computational Details

The calculations presented in this work were run using a series of python scripts based on the PyQuante suite [53]. The local spin-density approximation (LSDA) is used in pure and hybridized forms. Two hybrids of interest are considered, the “half-and-half” one, consisting of 50 % HF exchange, 50 % LSDA exchange, and 100 % LSDA correlation energies, we refer to this functional as LSDA-H. The second hybridized functional is denoted as “LSDA-75”, consisting of 75 % HF exchange, 25 % LSDA exchange, and 100 % correlation energies. All our bond-dissociation calculations were performed with the 6-31++G\*\* basis set. The convergence threshold for the (unrestricted) HF calculations is  $10^{-8}$  au, and for the  $t$ -amplitudes in the Q-eXp case  $10^{-6}$ . Tighter thresholds are possible, but were not needed in our simulations. The SG-2 grid is used to represent the XC potential and energy-density and to compute the XC energy. Reference calculations were performed with the Q-Chem computational chemistry software[54] for the standard KS calculations with the LSDA-H and -75 functionals, which are built using its user-defined density-functional interface. Reference unrestricted coupled cluster singles and doubles (UCCSD) were also carried out with Q-Chem. For Table 1 shown in next section, the minimum-energy geometries derive from MP2 calculations using aug-cc-pVQZ calculations that were performed with the NWChem program [55].

## 5 Results and Discussion

We begin our discussion with the  $\text{Ne}_2^+$  system. At dissociation of this diatomic molecule, the unrestricted Hartree-Fock (UHF) spin-symmetry process yields one atom as being neutral and the other one with positive charge. However, with a density functional such as the purely density-dependent XC LSDA, the energy levels of the atoms display an undesired behavior from the point of view of spin symmetry breaking: The lowest unoccupied  $p$  spin-level of the cation lies below that of the occupied  $p$ -shell of the neutral atom by about 18 eV, so the SCF algorithm will bias the ground-state mini-

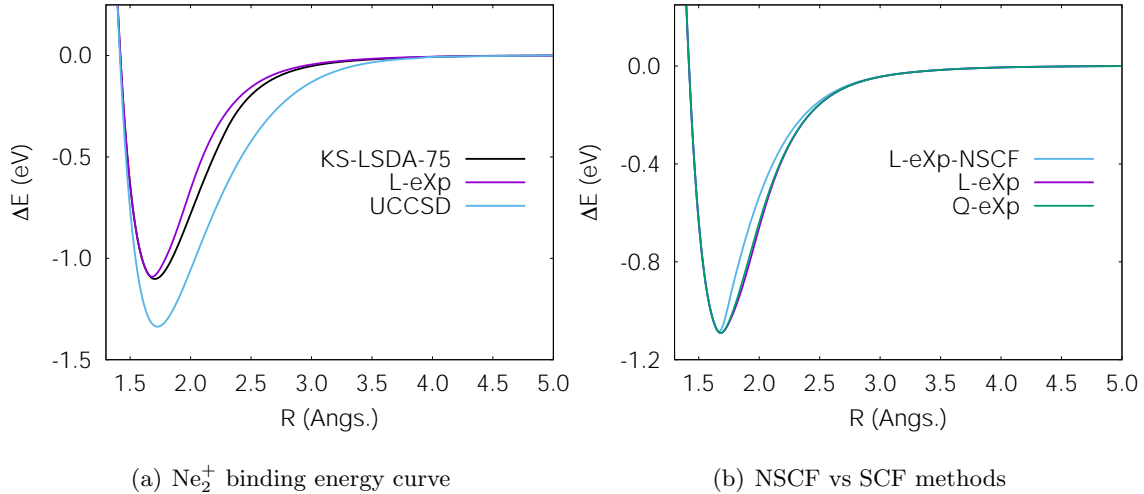


Figure 2: Performance of standard and eXp methods for the binding energy curve of  $\text{Ne}_2^+$ , where  $R$  denotes the internuclear distance: a), Comparison between a standard hybridized KS-LSDA calculation, self-consistent linearized eXp, and UCCSD. This curve shows that the linearized eXp calculation closely follows that of the standard KS-LSDA hybrid. b), Comparison between linearized and quadratic self-consistent eXp computations and a linearized non-self consistent simulation (all with  $\alpha = 0.1$  au). The NSCF calculation works well at equilibrium, repulsion, and dissociation, with some relatively small differences otherwise.

mization toward a charge-transfer configuration (where an electron is shared between the two atoms), delocalizing the positive charge and unphysically lowering the energy, as the  $\text{Ne} - \text{Ne}^+$  (neutral-cation) configuration energy configuration has a higher energy. The eXp method we propose can eliminate this problem in a pure LSDA calculation, but it requires strong regularization for moderately long distances between atoms. As mentioned before, which is well-known in the literature, the cause for charge delocalization is the self-interaction error. Therefore, it is possible to add HF exchange until the standard KS method performs appropriately at dissociation. This happens, for example, when the amount of HF exchange is 75 %, as shown in Figure 2.a, where our linearized eXp method reaches a size-consistent result, as well as the standard spin-symmetry-broken KS-LSDA-75 method. At this hybridization strength, however, the binding energy is underestimated with respect to UCCSD, which is more reliable in this case. But the L-eXp SCF result follows closely the standard KS-LSDA-75. Even at this level of hybridization, nevertheless, there are differences in energy level that are close to zero, when this occurs there are instabilities in the cluster amplitudes. For this reason, our calculation, L-eXp, includes a regularization number of 0.1 au. In previous work [42] we showed these eliminate iterative divergences while maintaining physical consistency with the parent methods used for comparison. As highlighted previously, an eXp calculation can proceed in a self-consistent fashion or not. In Figure 2.b we show that the linear and quadratic eXp SCF approaches yield very similar results,

whereas the linearized eXp method shows some deviations, but it remains physically meaningful with respect to the SCF calculations.

In our spin-symmetry breaking approach, at dissociation the left and right atomic systems are decoupled, so even if the energetics are unfavorable for the neutral configuration, a cluster amplitude where charge transfer takes place is not possible. For this reason, the charge delocalization is eliminated in the ground-state calculation. An example of such scenario is the functional we refer to as “LSDA-H” (50 % HF exchange, 50 % LSDA exchange, and 100 % correlation). Figure 3.a shows that the standard KS-LSDA-H technique yields a binding energy that is quite low at dissociation, due to the fractional-spin errors in the LSDA-H functional. The self-consistent linearized eXp method corrects this binding energy curve and ensures that the binding energy meets physical expectation, where it must tend to zero, as in the UHF and UCCSD results. As opposed to the LSDA-75 functional, LSDA-H in combination with L-eXp overestimates the binding energy around the equilibrium distance, hence a HF exchange weight between 50 and 75 % could give a better result for this matter, or a self-interaction corrected functional such as a Perdew-Zunger GGA. Further evidence of recovering size-consistency is provided in Figure 3.b, where the charge of UHF, L-eXp, and UCCSD tend to the expected symmetry broken result: one neutral Ne atom, and one Ne cation. The KS-LSDA-H result is unable to break the spin symmetry, resulting in the underestimation of the binding energy at long interatomic distances. This molecular system,  $\text{Ne}_2^+$  is challenging because it displays both charge and spin entanglement, quantum effects not encoded by conventional density functional approximations (for other difficult systems, see Ref. [56]). Because of this, the conventional approximations, even though give the right charges, predict erroneous energies and densities (although the charges are correct). Spin-symmetry is consistent with a collapse of the wavefunction at long distances, hence better energetics, and can serve as a starting basis for a re-symmetrization (not explored in this work) consistent with charge and spin entanglement. Despite the mentioned benefit of spin-symmetry breaking, in a LSDA-H LR TDDFT (linear response time-dependent DFT) procedure, the state of negative excitation energy associated to the spurious charge-transfer excitation would return. This is because of the inherent existence of such state which would manifest in the LR-TDDFT eigenvalue problem. But for higher amounts of HF exchange this effect can be eliminated, as discussed next for the LiF system.

We now discuss to the dissociation curve of lithium fluoride, which despite its relative simplicity as a diatomic molecule, it has been an important system in theoretical chemistry development; there are fluoride systems that are challenging in DFT method development [56]. The unregularized eXp-based self-consistent method can be unstable at moderately long distances between atoms, not a full dissociation. To understand an underlying reason for this behavior, separate (non-hybrid) LSDA calculations of the fluorine and lithium atoms show that the lowest unoccupied orbital of the F atom, with energy -10.3 eV, lies energetically below the highest occupied spin orbital of the Li atom, which has an orbital energy of -3.2 eV. Therefore, in case the electronic interaction is weak, the cluster operator during the SCF steps will attempt to transfer an electron from lithium to fluorine (similarly as in the  $\text{Ne}_2^+$  case), as it is favorable for the sake of minimizing the energy. This in turn causes an



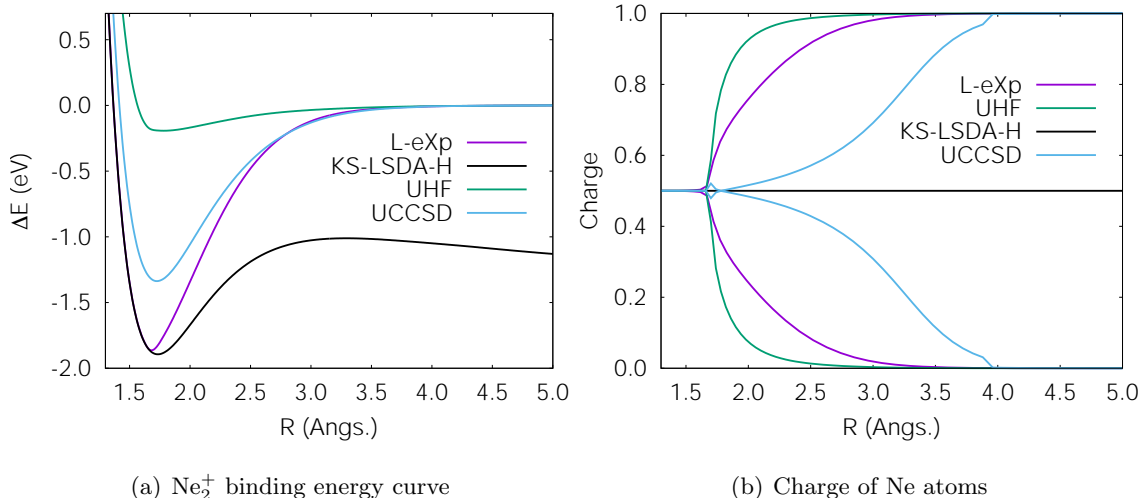


Figure 3: Binding energy of  $\text{Ne}_2^+$  and its atomic charges computed with different methods: a), Energies determined by linearized eXp method (LSDA-H functional), KS LSDA-H, UCCSD, and UHF. b), Atomic charges of each atom as determined by each method used in a).

eventual divergence because the system tries to force itself to be mostly dominated by a charge-transfer state. Such charge-transfer state of low energy is eliminated by setting the amount of HF exchange as 75 %, and by employing the linear or quadratic eXp method. However, at some intermediate distances between equilibrium and dissociation it requires  $\alpha = 0.2$  due to a few energy level differences ( $f_{aa} - f_{ii}$ ) being too close to zero. We employed a similar value for the hydrogen fluoride in past work, where we showed, again, that the results remain physically consistent. Even though not tested in this work because of its unavailability, in our opinion a very appealing improvement in this direction would be the inclusion of purely density-based self-interaction corrections.

To obtain a dissociation curve for LiF our method relies on the UHF reference. At quite long distances, as expected, the wavefunctions localized correctly. However, examination of the fully converged UHF solution of LiF reveals a sudden jump in the value of the  $\langle S^2 \rangle$  operator. The ground-state spin-square  $S^2$  value is thus non-analytic at a single point. In standard hybrid KS-LDA calculations this also introduces a non-differentiable point (or non-unique force value) in the dissociation curve, as shown in Figure 4.a. In contrast, however, in an eXp simulation such jump causes a similar unphysical step in the binding energy curve because the spin-decomposed exchange energy is sensitive to sudden changes in the spin-densities, and the solution to the DFT problem is pursued in a post-HF fashion; in other words, if the spin-density suddenly changes so could the exchange energies. This issue may be resolved if  $S^2$  is either forced to change smoothly, or is maintain fixed. To achieve this, we perform a fully converged UHF calculation at a relatively long distance, 8 Å, for example. The potential energy curve is then scanned by reducing step-by-step the internuclear distance  $R$ , where the UHF is updated only one time, Figure 4.b. Such procedure enables us to keep the  $S^2$  value of the system

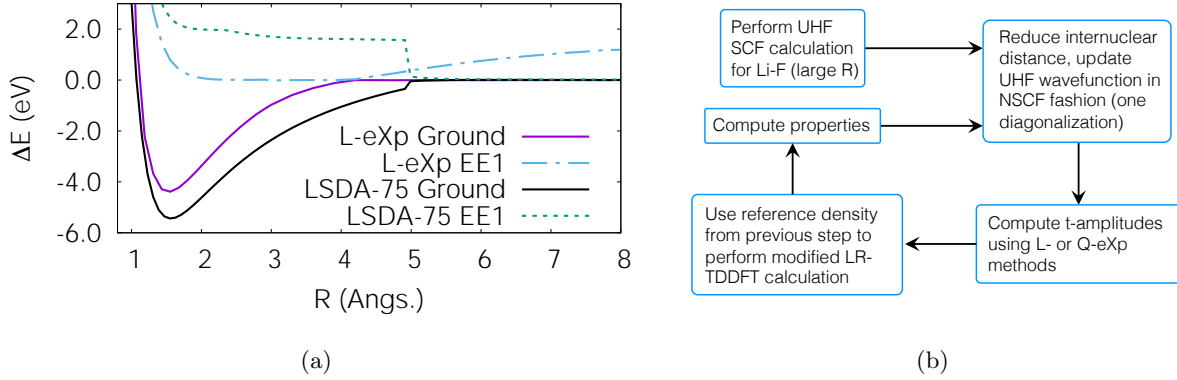


Figure 4: a), Binding energy curves of lithium fluoride computed with the linearized NSCF eXp method vs unrestricted standard KS LSDA-75, including the first excited state for both methods; “EE1” stands for the first excited state. a) Steps followed to compute ground- and excited-state energies.

nearly constant. This gives a symmetry-broken reference wave function in which each atom remains nearly neutral. Around the equilibrium distance of the system such reference wavefunction does not correspond to the HF wavefunction of the system. We therefore let the algorithm update the  $t$  amplitudes, but in the linear-response TDDFT step, we include a contribution from the symmetry-broken reference of the system; such change only requires a minor modification to the algorithms. Hence, the LR TDDFT solutions produce both the ground and excited states of the system. In our algorithm then, the LR TDDFT eigenvalues are given with respect to the reference. An auxiliary wave function in our methodology is of the form  $|\Psi_I\rangle = (X_0^I + \sum_{ai} X_{ai}^I \hat{a}^\dagger \hat{i}) e^{\hat{t}} |\Psi_0\rangle$ , where  $\Psi_0$  is in this case a NSCF UHF wavefunction, and  $\mathbf{X}^I = (X_0^I, \{X_{ai}^I\})$  is the so-called excitation vector corresponding to state  $I$ , which can either be the ground or an excited state. The energies  $\{\Omega_I\}$  and vectors  $\mathbf{X}^I$  with respect to the reference are found solving a LR-TDDFT eigenvalue problem of the form  $\mathbf{A}\mathbf{X}^I = \Omega_I\mathbf{X}^I$ , where  $\mathbf{A}$  is the Jacobian matrix in the excitation basis.

We find that the standard, symmetry broken (unrestricted), KS-LSDA-75 SCF result for LiF is size-consistent for the ground-state. However, there are two other issues that are present in this simulation: First, at dissociation, the charge-transfer configuration is not the first excited state, as expected, but instead a local excitation of the fluorine atom. Second, the unrestricted SCF LSDA-75 calculation also features a jump in the value of the squared spin operator, to which the excitation energies are sensitive too. Hence, even if the local fluorine excitation were ignored, a sudden jump remains. In Figure 4 we also show the NSCF L-eXp result (however, the other methods, NSCF L-eXp, SCF Q-eXp, or NSCF Q-eXp yield very similar dissociation energies due to the need for regularization). The L-eXp ground and first-excited state values are qualitatively correct. There is a point of near-degeneracy between the ground and excited states, and the charge transfer excitation is dominant at long distances. The

Table 1: Norm of dipole vectors and absolute value of ground-state energies computed with non-regularized L-eXp and Q-eXp, in NSCF and SCF ways, and using the (non-hybrid) LSDA XC functional, for a set of molecules at their equilibrium geometries. Values in atomic units.

Molecule	Q-eXp SCF		L-eXp SCF		Q-eXp Non-SCF		L-eXp Non-SCF	
	Dipole	Total Energy	Dipole	Total Energy	Dipole	Total Energy	Dipole	Total Energy
H <sub>2</sub> O	0.887	75.868168	0.887	75.868168	0.882	75.868080	0.882	75.868078
CO	0.079	112.416288	0.080	112.416288	0.496	112.398708	0.505	112.39811
CH <sub>3</sub> OH	0.750	114.787583	0.749	114.787583	0.709	114.783330	0.708	114.783279
CH <sub>3</sub> F	0.772	138.717566	0.772	138.717566	0.649	138.708433	0.647	138.708284
HCN	1.190	92.610848	1.190	92.610848	1.017	92.607709	1.014	92.607646
H <sub>3</sub> O <sup>+</sup>	0.677	76.137484	0.677	76.137484	0.680	76.137398	0.680	76.137398
OH <sup>-</sup>	0.731	75.249223	0.731	75.249223	0.689	75.243512	0.689	75.243331
LiH	2.211	7.911541	2.211	7.911541	2.107	7.910796	2.105	7.910774
LiH <sub>2</sub> <sup>+</sup>	1.231	8.284455	1.230	8.284455	1.221	8.284399	1.221	8.284399

value of this excitation also agrees with FCI calculations, as well as the fact that the gap between the ground and first excited state is quite small around the anticrossing point. However, the ground-state binding energy at equilibrium is underestimated, as well as the internuclear distance at the anticrossing point. Nonetheless, these features could be fixed, we believe, by an improved density functional approximation, specially suited for this type of physical situation.

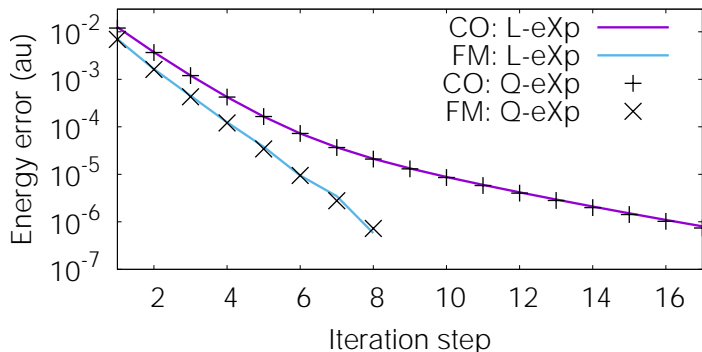


Figure 5: Convergence of the linearized and quadratic eXp methods for the the minimum-energy geometry of carbon monoxide and fluoromethane.

We now discuss the interplay between the different ways to perform calculations: The Q- and L-eXp methods with and without self-consistency. It is important to remark that even though a calculation based on cluster operators can be non-self-consistent, the full (self-consistent) Hartree-Fock orbitals are employed as the starting basis in this present analysis (summarized by Table 1). As an example, we choose the carbon monoxide and fluoromethane molecules at the minimum ground-state-energy

configuration and consider the convergent behavior of L- and Q-eXp. Figure 5 shows that only few steps are required to converge the eXp wavefunctions for an energy threshold of  $10^{-6}$  au. For CO, L- and Q-eXp behave nearly identically, where a quite small difference is observed for fluoromethane. Our method does not require too many steps because a Hartree-Fock calculation was performed prior to the SCF eXp simulation. In the molecular set considered, as shown in Table 1, the self-consistent L- and Q-eXp techniques perform quite similarly. Some differences are noticeable, however, when the cluster amplitudes are determined non-self-consistently, especially for CO and CH<sub>3</sub>F. These two molecules require the most SCF steps, which correlates well with the differences seen in the NSCF calculations. If regularization were applied, we would expect fewer SCF steps, but not necessarily more agreement with the unregularized NSCF calculations, unless these are regularized as well. For this set of molecules the NSCF step in general improves the properties of interest. This may suggest then that the NSCF procedures can be of use for practical electronic structure calculations, particularly in cases where computational savings are needed. An eXp NSCF calculation may also be performed with regularization, if required. The issue of instabilities in cluster amplitudes is not inherent to our method only, but it is common in CC theory in general, when energy differences are very small, for example in semi-metallic systems. But with some form of regularization it can be eliminated.

## 6 Conclusions

As an alternative to the standard approach to solve the Kohn-Sham DFT electronic structure problem, we investigated approximated solutions by means of singles-based cluster operators and amplitudes. These solutions could serve as a basis for the development of algorithms free of the delocalization error, with a broader view of electronic excitations, and capable of delivering size consistency in general (whether the auxiliary Hamiltonian of the system is single- or multi-particle in principle). We found several potential approaches for the use of this operator in the calculation of alternative single-particle wavefunctions, thus offering flexible pathways for practical calculations. The linear approach seems to be quite convenient due its relative accuracy and computational cost. Even though the cluster operator in DFT can be of use in numerical procedures, its applicability to systems that are inherently of multireference character (from a WFT point of view) is an unexplored subject, but clearly encouraging. In this direction, the theoretical procedures presented here may serve for the formulation of electronic structure models that either couple with automated approaches, or with techniques that rely on localization/symmetry-breaking of orbitals in order to describe challenging quantum systems. As it is well-known, different systems need different degrees of self-interaction corrections. For this reason, connections with quantum embedding [57] could be beneficial to improve accuracy by assigning different exchange mixtures to different subsystems in a large molecular system. This, in conjunction with eXp calculations, could be of interest for density functional calculations with expanded capabilities.

## 7 Acknowledgment

G.J. and M.A.M. acknowledge funding from the National Science Foundation Research Experiences for Undergraduates (REU) Program (award CHE-1852214). M.A.M and J.M.M.T. thank Montana State University – Bozeman for startup support.

## References

- [1] Walter Kohn and Lu Jeu Sham. Self-consistent equations including exchange and correlation effects. *Phys. Rev.*, 140(4A):A1133, 1965.
- [2] Kieron Burke. Perspective on density functional theory. *J. Chem. Phys.*, 136(15):150901, 2012.
- [3] E Chamorro and P Pérez. Chemical reactivity within the spin-polarized framework of density functional theory. In P K Chattaraj and D Chakraborty, editors, *Chemical Reactivity in Confined Systems: Theory, Modelling and Applications*, pages 135–165. Wiley Online Library, 2021.
- [4] Per EM Siegbahn, Margareta RA Blomberg, and Shi-Lu Chen. Significant van der waals effects in transition metal complexes. *J. Chem. Theor. Comput.*, 6(7):2040–2044, 2010.
- [5] John P Perdew, Robert G Parr, Mel Levy, and Jose L Balduz Jr. Density-functional theory for fractional particle number: Derivative discontinuities of the energy. *Phys. Rev. Lett.*, 49(23):1691–1694, 1982.
- [6] Dávid Mester and Mihály Kállay. Charge-transfer excitations within density functional theory: How accurate are the most recommended approaches? *J. Chem. Theor. Comput.*, 18(3):1646–1662, 2022.
- [7] Eduard Matito and Miquel Solà. The role of electronic delocalization in transition metal complexes from the electron localization function and the quantum theory of atoms in molecules viewpoints. *Coordin. Chem. Rev.*, 253(5-6):647–665, 2009.
- [8] Marcus Lundberg and Per EM Siegbahn. Quantifying the effects of the self-interaction error in dft: When do the delocalized states appear? *J. Chem. Phys.*, 122(22):224103, 2005.
- [9] A Otero-De-La-Roza, Erin R Johnson, and Gino A DiLabio. Halogen bonding from dispersion-corrected density-functional theory: The role of delocalization error. *J. Chem. Theory Comput.*, 10(12):5436–5447, 2014.
- [10] Jochen Autschbach and Monika Srebro. Delocalization error and “functional tuning” in kohn–sham calculations of molecular properties. *Acc. Chem. Res.*, 47(8):2592–2602, 2014.

- [11] Yingkai Zhang and Weitao Yang. A challenge for density functionals: Self-interaction error increases for systems with a noninteger number of electrons. *J. Chem. Phys.*, 109(7):2604–2608, 1998.
- [12] P Mori-Sánchez, AJ Cohen, and W Yang. Many-electron self-interaction error in approximate density functionals. *J. Chem. Phys.*, 125(20):201102, 2006.
- [13] Oleg A Vydrov, Gustavo E Scuseria, and John P Perdew. Tests of functionals for systems with fractional electron number. *J. Chem. Phys.*, 126(15):154109, 2007.
- [14] Aron J Cohen, Paula Mori-Sánchez, and Weitao Yang. Insights into current limitations of density functional theory. *Science*, 321(5890):792–794, 2008.
- [15] Sebastian Dick and Marivi Fernandez-Serra. Machine learning accurate exchange and correlation functionals of the electronic density. *Nat. Commun.*, 11(1):1–10, 2020.
- [16] Ryan Pederson, Bhupalee Kalita, and Kieron Burke. Machine learning and density functional theory. *Nat. Rev. Phys.*, 4(6):357–358, 2022.
- [17] James Kirkpatrick, Brendan McMorro, David HP Turban, Alexander L Gaunt, James S Spencer, Alexander GDG Matthews, Annette Obika, Louis Thiry, Meire Fortunato, David Pfau, et al. Pushing the frontiers of density functionals by solving the fractional electron problem. *Science*, 374(6573):1385–1389, 2021.
- [18] Jorge Nochebuena, Sehr Naseem-Khan, and G Andrés Cisneros. Development and application of quantum mechanics/molecular mechanics methods with advanced polarizable potentials. *Wiley Interdiscip. Rev.: Comput. Mol. Sci.*, 11(4):e1515, 2021.
- [19] Caio A Custódio, Érica R Filletti, and Vivian V França. Artificial neural networks for density-functional optimizations in fermionic systems. *Sci. Rep.*, 9(1):1–7, 2019.
- [20] Junmian Zhu, Bobby G Sumpter, Stephan Irle, et al. Artificial neural network correction for density-functional tight-binding molecular dynamics simulations. *MRS Commun.*, 9(3):867–873, 2019.
- [21] Konstantin Gubaev, Evgeny V. Podryabinkin, Gus L.W. Hart, and Alexander V. Shapeev. Accelerating high-throughput searches for new alloys with active learning of interatomic potentials. *Comput. Mater. Sci.*, 156:148–156, 2019. ISSN 0927-0256. doi: <https://doi.org/10.1016/j.commatsci.2018.09.031>. URL <https://www.sciencedirect.com/science/article/pii/S0927025618306372>.
- [22] Chandramouli Nyshadham, Matthias Rupp, Brayden Bekker, Alexander V. Shapeev, Tim Mueller, Conrad W. Rosenbrock, Gábor Csányi, David W. Wingate, and Gus L. W. Hart.

- Machine-learned multi-system surrogate models for materials prediction. *npj Comput. Mater.*, 5(1):51, Apr 2019. ISSN 2057-3960. doi: 10.1038/s41524-019-0189-9. URL <https://doi.org/10.1038/s41524-019-0189-9>.
- [23] Yunxing Zuo, Chi Chen, Xiangguo Li, Zhi Deng, Yiming Chen, Jörg Behler, Gábor Csányi, Alexander V. Shapeev, Aidan P. Thompson, Mitchell A. Wood, and Shyue Ping Ong. Performance and cost assessment of machine learning interatomic potentials. *J. Phys. Chem. A*, 124:731–745, 1 2020. ISSN 15205215. doi: 10.1021/acs.jpca.9b08723.
- [24] Alexander V. Shapeev. Moment tensor potentials: A class of systematically improvable interatomic potentials. *Multiscale Model. Simul.*, 14:1153–1173, 2016. ISSN 15403467. doi: 10.1137/15M1054183.
- [25] Jörg Behler. Perspective: Machine learning potentials for atomistic simulations. *J. Chem. Phys.*, 145(17):170901, 2016. doi: 10.1063/1.4966192. URL <https://doi.org/10.1063/1.4966192>.
- [26] I. I. Novoselov, A. V. Yanilkin, A. V. Shapeev, and E. V. Podryabinkin. Moment tensor potentials as a promising tool to study diffusion processes. *Comput. Mater. Sci.*, 164:46–56, 6 2019. ISSN 09270256. doi: 10.1016/j.commatsci.2019.03.049.
- [27] V. V. Ladygin, P. Yu Korotaev, A. V. Yanilkin, and A. V. Shapeev. Lattice dynamics simulation using machine learning interatomic potentials. *Computational Materials Science*, 172:109333, 2 2020. ISSN 09270256. doi: 10.1016/j.commatsci.2019.109333.
- [28] Bohayra Mortazavi, Ivan S. Novikov, Evgeny V. Podryabinkin, Stephan Roche, Timon Rabczuk, Alexander V. Shapeev, and Xiaoying Zhuang. Exploring phononic properties of two-dimensional materials using machine learning interatomic potentials. *Appl. Mater. Today*, 20:100685, 9 2020. ISSN 23529407. doi: 10.1016/j.apmt.2020.100685.
- [29] Bohayra Mortazavi, Evgeny V. Podryabinkin, Ivan S. Novikov, Stephan Roche, Timon Rabczuk, Xiaoying Zhuang, and Alexander V. Shapeev. Efficient machine-learning based interatomic potentials for exploring thermal conductivity in two-dimensional materials. *JPhys Mater.*, 3:02LT02, 4 2020. ISSN 25157639. doi: 10.1088/2515-7639/ab7cbb.
- [30] Juan M. Marmolejo-Tejada and Martín A. Mosquera. Thermal properties of single-layer mos<sub>2</sub>-ws<sub>2</sub> alloys enabled by machine-learned interatomic potentials. *Chem. Commun.*, 58:6902–6905, 2022. doi: 10.1039/D2CC02519A. URL <http://dx.doi.org/10.1039/D2CC02519A>.
- [31] Fritz Coester. Bound states of a many-particle system. *Nucl. Phys.*, 7:421–424, 1958.
- [32] Fritz Coester and Hermann Kümmel. Short-range correlations in nuclear wave functions. *Nucl. Phys.*, 17:477–485, 1960.

- [33] Jiří Čížek. On the correlation problem in atomic and molecular systems. calculation of wave-function components in ursell-type expansion using quantum-field theoretical methods. *J. Chem. Phys.*, 45(11):4256–4266, 1966.
- [34] Jiří Čížek. On the use of the cluster expansion and the technique of diagrams in calculations of correlation effects in atoms and molecules. *Adv. Chem. Phys.*, pages 35–89, 1969.
- [35] Hendrik J Monkhorst. Calculation of properties with the coupled-cluster method. *Int. J. Quantum Chem.*, 12(S11):421–432, 1977.
- [36] D Mukherjee and PK Mukherjee. A response-function approach to the direct calculation of the transition-energy in a multiple-cluster expansion formalism. *Chem. Phys.*, 39(3):325–335, 1979.
- [37] K Emrich. An extension of the coupled cluster formalism to excited states (i). *Nucl. Phys. A*, 351(3):379–396, 1981.
- [38] K Emrich. An extension of the coupled cluster formalism to excited states:(ii). approximations and tests. *Nucl. Phys. A*, 351(3):397–438, 1981.
- [39] Somnath Ghosh and Debashis Mukherjee. Use of cluster expansion techniques in quantum chemistry. a linear response model for calculating energy differences. *Proc. Indian Acad. Sci. (Chem. Sci.)*, 93(6):947–963, 1984.
- [40] John F Stanton and Rodney J Bartlett. The equation of motion coupled-cluster method. a systematic biorthogonal approach to molecular excitation energies, transition probabilities, and excited state properties. *J. Chem. Phys.*, 98(9):7029–7039, 1993.
- [41] Rodney J Bartlett and Monika Musiał. Coupled-cluster theory in quantum chemistry. *Rev. Mod. Phys.*, 79(1):291–352, 2007.
- [42] Martín A Mosquera. Density functional calculations based on the exponential ansatz. *J. Phys. Chem. A*, 125(39):8751–8763, 2021.
- [43] Lars Goerigk and Stefan Grimme. Double-hybrid density functionals. *WIREs Comput. Mol. Sci.*, 4(6):576–600, 2014.
- [44] Jeng-Da Chai and Martin Head-Gordon. Long-range corrected double-hybrid density functionals. *J. Chem. Phys.*, 131(17):174105, 2009.
- [45] Tobias Schwabe and Stefan Grimme. Double-hybrid density functionals with long-range dispersion corrections: Higher accuracy and extended applicability. *Phys. Chem. Chem. Phys.*, 9(26):3397–3406, 2007.



- [46] Karol Kowalski and Marat Valiev. Extensive regularization of the coupled cluster methods based on the generating functional formalism: Application to gas-phase benchmarks and to the  $\text{sn}_2$  reaction of  $\text{chcl}_3$  and  $\text{oh}^-$  in water. *J. Chem. Phys.*, 131(23):234107, 2009.
- [47] Karol Kowalski and Peng-Dong Fan. Generating functionals based formulation of the method of moments of coupled cluster equations. *J. Chem. Phys.*, 130(8):084112, 2009.
- [48] Andrew G Taube and Rodney J Bartlett. Rethinking linearized coupled-cluster theory. *J. Chem. Phys.*, 130(14):144112, 2009.
- [49] Keith V Lawler, John A Parkhill, and Martin Head-Gordon. Penalty functions for combining coupled-cluster and perturbation amplitudes in local correlation methods with optimized orbitals. *Mol. Phys.*, 106(19):2309–2324, 2008.
- [50] Chenchen Song and Todd J Martínez. Analytical gradients for tensor hyper-contracted mp2 and sos-mp2 on graphical processing units. *J. Chem. Phys.*, 147(16):161723, 2017.
- [51] Luke W Bertels, Joonho Lee, and Martin Head-Gordon. Third-order møller–plesset perturbation theory made useful? choice of orbitals and scaling greatly improves accuracy for thermochemistry, kinetics, and intermolecular interactions. *J. Phys. Chem. Lett.*, 10(15):4170–4176, 2019.
- [52] Stefano Battaglia, Lina Fransén, Ignacio Fdez. Galván, and Roland Lindh. Regularized caspt2: an intruder-state-free approach. *J. Chem. Theor. Comput.*, 2022.
- [53] R P Muller. *Python Quantum Chemistry (PyQuante) Program, version 1.6.5*, <http://pyquante.sourceforge.net/>, 2007.
- [54] Yihan Shao, Zhengting Gan, Evgeny Epifanovsky, Andrew TB Gilbert, Michael Wormit, Joerg Kussmann, Adrian W Lange, Andrew Behn, Jia Deng, Xintian Feng, et al. Advances in molecular quantum chemistry contained in the q-chem 4 program package. *Mol. Phys.*, 113(2):184–215, 2015.
- [55] Marat Valiev, Eric J Bylaska, Niranjana Govind, Karol Kowalski, Tjerk P Straatsma, Hubertus JJ Van Dam, Dunyou Wang, Jarek Nieplocha, Edoardo Apra, Theresa L Windus, and W A de Jong. Nwchem: A comprehensive and scalable open-source solution for large scale molecular simulations. *Comput. Phys. Commun.*, 181(9):1477–1489, 2010.
- [56] Tim Gould and Stephen G Dale. Poisoning density functional theory with benchmark sets of difficult systems. *Phys. Chem. Chem. Phys.*, 24(11):6398–6403, 2022.
- [57] Leighton O Jones, Martín A Mosquera, George C Schatz, and Mark A Ratner. Embedding methods for quantum chemistry: Applications from materials to life sciences. *J. Am. Chem. Soc.*, 142(7):3281–3295, 2020.